



Cenozoic pelagic accumulation rates and biased sampling of the deep sea record

Johan Renaudie¹ and David B. Lazarus¹

¹Museum für Naturkunde, Leibniz-Institut für Evolutions- und Biodiversitätsforschung, Invalidenstrasse 43, 10115 Berlin, Germany

Correspondence: Johan Renaudie (lecoryphee@googlemail.com)

Abstract. Global weathering is a primary control of the earth's climate over geologic time scales: converting atmospheric pCO_2 into dissolved bicarbonate; with carbon sequestration by marine plankton as carbonate and organic carbon on the ocean floor. The accumulation rate of pelagic marine biogenic sediments are thus a measure of weathering history. Previous studies of Cenozoic pelagic sedimentation have yielded contrasting results, though most show a dramatic rise (up to 6 times) in rates over the Cenozoic. This contrasts with model expectations for approximate steady state in weathering, pCO_2 , and sequestration over time. Here we show that the Cenozoic record of sedimentation recovered by deep sea drilling has a strong, systematic bias towards lower rates of sedimentation with increasing age. When this bias is removed accumulation rates are shown to actually decline by ca 2 times over the Cenozoic. When accumulation area however is adjusted for changes in available deposition area, global weathering is shown to have nearly doubled at the Eocene-Oligocene boundary, but was otherwise essentially constant. Compilations of other metrics correlated to sedimentation rate (e.g. productivity, biotic composition) also must have a strong age bias, which will need to be considered in future paleoceanographic studies.

1 Introduction

The rate of global chemical weathering is a key parameter in many areas of earth system science. In the Cenozoic, most of the dissolved ions - the products of weathering - are thought to have been sequestered as biogenic skeletal materials, and mostly by burial of oceanic plankton in deep sea sediments, with coastal sequestration and reverse weathering playing a secondary role (Ridgwell and Hargreaves, 2007; Tréguer and De La Rocha, 2013). Many Cenozoic weathering proxies, using element isotope ratios from deep sea sediments that reflect differential continental vs oceanic sources (e.g. Sr, Os, Li and Be), show patterns implying, albeit complicated by multiple debated parameterizations, moderately increasing, or even constant rates of weathering, with change from lower to higher rates near the Eocene-Oligocene boundary, and/or the late Neogene (Raymo et al., 1988; Goddérís and François, 1995; Peucker-Ehrenbrink et al., 1995; Lear et al., 2003; Dalai et al., 2006; Misra and Froelich, 2012). Deep sea pelagic sediment accumulation rate (SAR), the most direct measurement of Cenozoic weathering output, vary enormously by location (Lisitzin, 1972). Global compilations that compensate for geographic variation however show a nearly exponential SAR increase over the Cenozoic. Though many studies rely on early compilations of limited DSDP era data (Davies et al., 1977; Worsley and Davies, 1979; Hay et al., 1988), even more recent estimates (Westacott et al., 2021),



25 based on a selection of higher quality sections (Lisiecki and Raymo, 2005; Cramer et al., 2009) show a near continuous, ca
6X increase in SAR over Cenozoic (Westacott et al., 2021). This discrepancy has been a major challenge to understanding
Cenozoic weathering and geochemical cycling.

The apparent increase in pelagic SAR has been suggested (Willenbring and Jerolmack, 2016) to be an artifact of the ‘Sadler
effect’ (Sadler, 1981), based on a shallow water sedimentation model of extensive hiatuses, a hierarchy of ‘ever more and
30 longer hiatuses’ as measurement time interval increases, and decreasing age measurement resolution with increasing geologic
age (Sadler, 1981). These factors yield apparent decreasing SAR in many types of stratigraphic sections with increasing age
and time scale of measurement (Sadler, 1981). In the deep sea, with usually continuous (on scales > 1 yr) if variable rate rain
from surface productivity and a much lower energy benthic sediment erosion regime, one would not expect to see strong Sadler
effect. Sections in paleoceanographic studies are frequently reported as nearly complete at biostratigraphic zone to orbital
35 tuning resolution (ca 500-20 kyr), typically with only a few, limited duration hiatuses. Pelagic microfossil biostratigraphic
zones are also similar in resolution over the entire Cenozoic (Vandenberghe et al., 2012; Hilgen et al., 2012). Lastly there was
no observed effect in the original study of Sadler in his (limited) deep sea data on any time scale superior to ca .5 my (Sadler,
1981). It is thus important to test if the Sadler effect is actually responsible for the observed several fold increase in Cenozoic
pelagic sedimentation rates. If the deep sea pelagic sedimentary record is not (strongly) biased by hiatus-driven measurement
40 scale artifacts, then the major increase in apparent rate over Cenozoic means either that geochemical proxies are somehow
wrong and rate has changed exponentially, or that some other factors are biasing the Cenozoic deep sea record.

Here we examine 1) hiatus biases affecting apparent SAR; 2) whether SAR (excluding hiatuses) decline with increasing age,
3) demonstrate a new mechanism - drilling bias - that is responsible for the apparent decline in SAR, 4) apply this insight to
determine Cenozoic weathering rates, and 5) briefly discuss the broader implications of drilling bias for paleoceanographic
45 research.

2 Material and Methods

2.1 LSR and SAR compilation.

The Linear Sedimentation Rates (hereafter LSR) computed here derive from a much more comprehensive, and relatively
unbiased selection of deep sea drilling sites than has been used in prior studies. Specifically we use the age models for all
50 479 sites produced and revised, primarily by the authors over a period of nearly 30 years, for the Neptune (NSB) database
(Lazarus, 1992, 1994; Lazarus et al., 1995; Renaudie et al., 2020). Sites selected for inclusion in NSB meet the criteria of
adequate recovery and sufficient information to construct a usable age model (meaning in practice at least adequate microfossil
data) but otherwise are not selected for specific sedimentation criteria, or age intervals, and include mostly sites from the
qualitatively better recovered ODP and IODP phases of the deep sea drilling programs. LSR at each site was computed every
55 10 kyrs from 66 to 0 Ma; and global median LSR was computed, along with its interquartile range (IQR (Tukey, 1977)), based
on all sites. The moisture and density measurements for each site were extracted from the NGDC archive CD-ROM (National
Geophysical Data Center, 2000, 2001), Janus (Mithal and Becker, 2006) and LIMS databases (lim, 2016). Densities for each

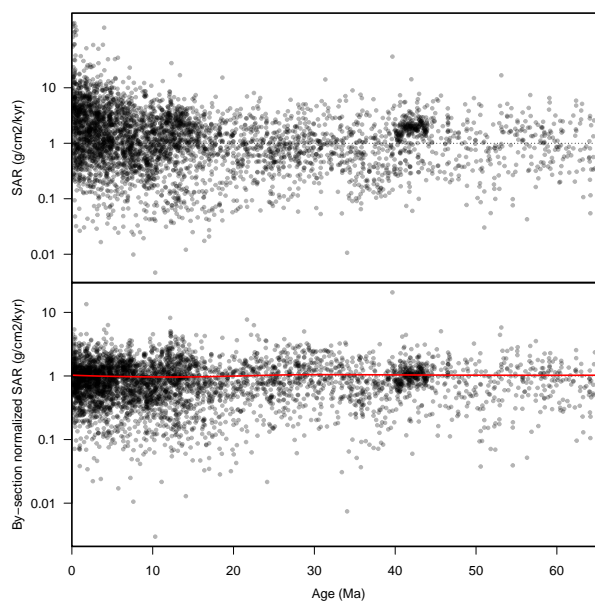


Figure 1. Top Panel: SAR through time for each individual section of age model.

Bottom Panel: Observed SAR normalized by section with trend over time (LOESS; in red), showing the absence of a global pattern, on a section by section basis, toward increasing SAR over the Cenozoic.

site were used to transform each site LSR into Sediment Accumulation Rates (hereafter SAR), expressed in $g.cm^{-2}.kyr^{-1}$. These were compiled globally the same way as the global LSR was (see Figure 2). As neither LSR or SAR distributions follow a normal distribution, medians are reported here rather than means; however for the purposes of direct comparison with the published literature which did use overwhelmingly means rather than medians, means are also reported and illustrated in the Supplementary Material.

Median LSR and SAR were computed for each ocean basin (see Figure 7). The dataset comprises 220 holes for the Atlantic basin, 187 for the Pacific, 54 for the Indian and 12 for the Southern Ocean. To correct for geographical sampling bias, we recalculated the global SAR curve as an area-weighted composite of the regional curves. The result is shown, together with the simple global median curve, on Figure 7. The area of the ‘red clay’-free oceans (i. e. 74.2% of the Atlantic, 51% of the Pacific and 74.7% of the Indian Ocean (Rothwell, 2016)) are used instead of their full area, as the area covered in red clay is not representative of pelagic sedimentation, being mostly eroded but unweathered terrigenous dust sized material (Glasby, 1991).

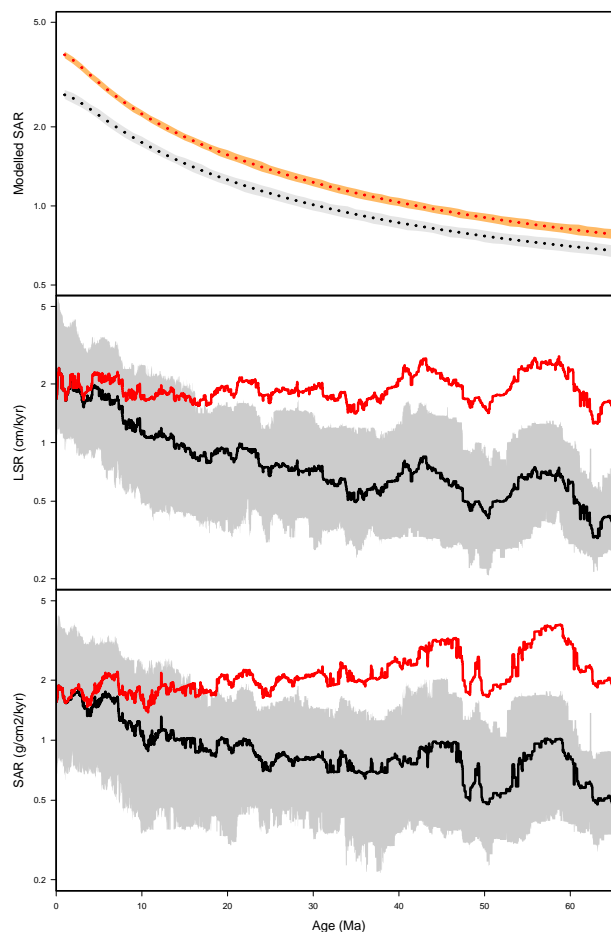


Figure 2. Top Panel: Bias towards lower apparent sedimentation rate in older time intervals in drilled sections. Results from a model where there is no actual change in local accumulation rate over time, rates however vary geographically. These sediments are then sampled by drilling sites with a randomly chosen drilling depth, drawn from the distribution of drilling depths of all deep sea drilling program sites. The *apparent* sedimentation rate over time compiled from the drilled sections is not constant but declines with increasing geological age, in part due to sediment compaction, but primarily by biased sampling of the older record. In black, median SAR averaged over 1000 runs (in grey, full extent of the various runs) and in red, mean SAR averaged over the same runs (in orange, full extent).

Middle and Bottom Panel: Linear Sedimentation Rates (middle; expressed in $cm.kyr^{-1}$) and Accumulation Rates (bottom; expressed in $g.cm^{-2}.kyr^{-1}$). Black: distribution as observed in our global dataset (solid line: median; grey shading: interquartile range); Red: median sedimentation and accumulation rates corrected for drilling bias using the result of the model). Rates are on a log-scale.

70 2.2 Bias testing and modelling.

Drilling depths, local SARs, hiatus frequencies and durations for model sections are all taken from the NSB database (Renaudie et al., 2020, 2023). Age models are generally accurate to ca 0.5 Myr, although some poor models are significantly less precise

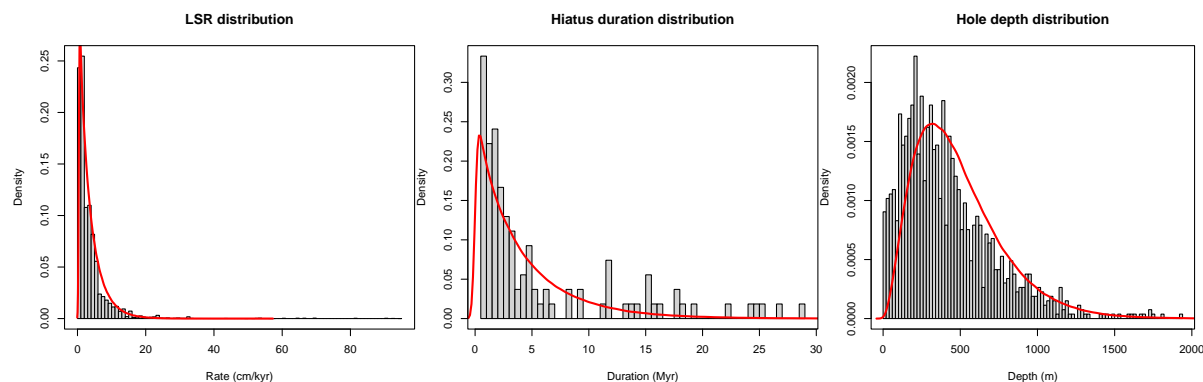


Figure 3. First Panel: Histogram of observed values of Pleistocene LSR in grey and density distribution of the modelled LSR (a translated Weibull distribution of shape $\kappa = 0.95$, scale $\lambda = 3.34$ and location $\theta = 0.4$) in red. Second Panel: Histogram of observed hiatuses duration in grey and density of the modelled distribution (a Weibull distribution of shape $\kappa = 0.95$ and scale $\lambda = 4$). Third panel: Histogram of DSDP, ODP and IODP hole depths in grey and density of the modelled distribution (a Gamma distribution of shape $\kappa = 2.93$ and scale $\theta = 166.97$).

(> 1 Myr errors) and others (orbitally tuned sections) are much more precise (ca 40 kyr) (Renaudie et al., 2020; Smith et al., 2023).

75 We first examine potential magnitude of the Sadler effect by computing hiatus frequencies and durations vs intervals of sediment accumulation in deep sea sections, and by creating a density plot of SAR vs time span over which the SAR was measured from the NSB data (see Supplementary Material). We then calculate by-section normalized change in sedimentation rates vs geologic age in intervals with sedimentation to see if older time intervals, corrected for between site differences in local rates, show a decline in relative rate with increasing geologic age (see Figure 1).

80 Despite attempts to pinpoint biases in such compilations (Whitman and Davies, 1979), one aspect has not been explored yet: the bias introduced by the drilling process itself on the dataset. Drilling is limited in depth (due to technical, cost and time constraints). To capture the same time interval one would have to drill significantly deeper at high, than at a low sedimentation rate location. The complex history of ocean drilling, with its originally poor knowledge of local ocean sedimentation rates, and changing geologic time interval priority targets (geologically young, high sedimentation rate sections; low sedimentation rate sections overlying geologically old target intervals, etc; Imbrie et al., 1987; Coffin et al., 2001), has not however, over the course of the programs, systematically adjusted drilling depths on a global scale to compensate for differing sedimentation rates. Thus, in global compilations of deep sea drilling data, drilling depths can be treated as being random to local sedimentation rate. The important consequence is that the older the sediments recovered are, the more likely they are to be represented only by low sedimentation rate sites, as penetration to older aged sediments is more likely when the local sedimentation rate is low.

90 To correct for the drilling bias problem, we modelled what the bias would be in an imaginary situation where individual sites have constant accumulation rate through time (see Supplementary Code). Each modelled site has a total drilling depth

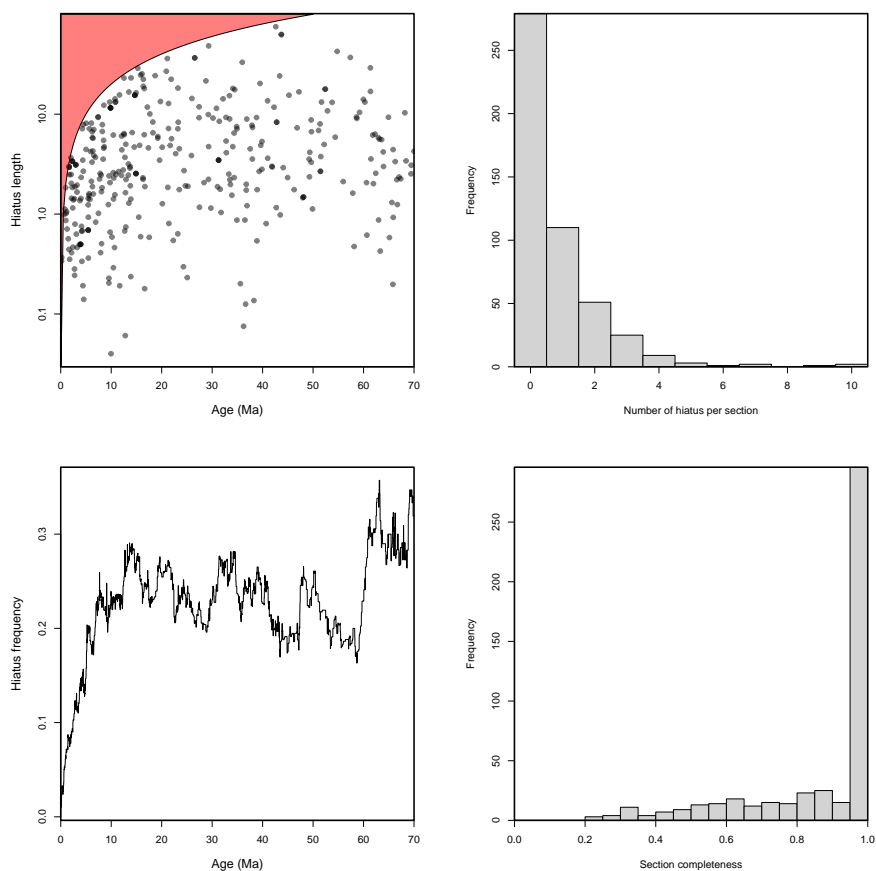


Figure 4. Top Left Panel: Hiatus length through time (age of hiatus is its median age; in red is the area of the plot that thus can not be populated). Bottom Left Panel: Hiatus frequency through time (i. e. what proportion of sections ranging through a given time interval do not recover that particular time interval). Top Right Panel: Histogram of number of hiatus per section. Bottom Right Panel: Histogram of section completeness (i. e. given a hole whose bottom core is at age x, what percentage of those x Ma were recovered).

picked from a distribution matching actual distribution of site depths (see Figure 3), and a fixed accumulation rate picked from distribution approaching the closest the distribution of sedimentation rates seen in late Pleistocene, i. e. the one time interval not much affected by compaction or by the drilling bias. Finally, to include the Sadler effect, hiatuses of random length are added randomly with a probability equal to the occurrence ratio of hiatuses in our age model dataset. The distribution of observed mean LSR for each time interval over the Cenozoic is averaged from sets of modelled sites (1,000 per run). The output of our model calculates the bias due to depth-limited drilling of geographically highly variable LSR sections in the absence of any time dependent change in LSR. Details of the model is given in the Supplementary Material.

95

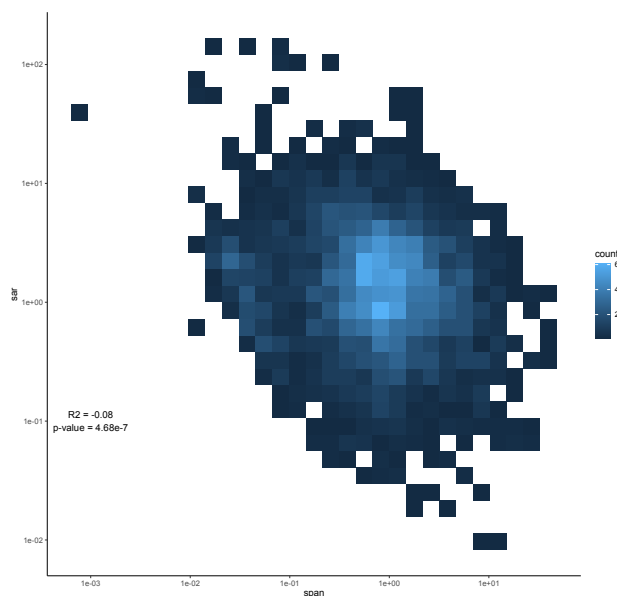


Figure 5. Density plot relationship between computed SAR and time span of the age model segment over which it was computed.

2.3 Unbiased SAR curve and global sediment flux history.

100 The inverse of the resulting modelled LSR vs geologic age curve is used as a correction factor on the NSB-based LSR and SAR compilation (see Figure 2 and 7).

Lastly, we computed Cenozoic change in pelagic sedimentation areas (in millions of km^{-2} ; Figure 8), simplified as the marine areas above the carbon compensation depth (hereafter CCD), using previously published estimates of CCD in the Equatorial Pacific (Pälike et al., 2012) (taken here as a rough estimate for global CCD changes) and paleotopographic maps
105 (Scotese and Wright, 2018; Kocsis and Raja, 2020). Using these area estimates and the new composite unbiased SAR compilation we produced an estimate of the total global sediment flux history (in $Pg.yr^{-1}$), though over the last 55 million years only, as the previous 11 million years are not covered by the published CCD estimate (Figure 8).

3 Results

3.1 By-section analyses of hiatuses and sedimentation.

110 The relation of SAR to time span of measurement is very weak, with an R2 of only -0.08 (Figure 5). Unrecognized hiatuses in longer age model segments (e.g. in poorer age models) thus do not have a significant effect on SAR. Nor do age model segment spans increase with geologic age (Figure 4). Age model hiatuses (>0.5 my) in NSB deep sea sediment sections are relatively rare (median 0, mean 0.93 hiatuses/section; Figure 4). Most are of fairly short duration (median 2.98 Myr), though there is an extended tail of rare, longer duration hiatuses, thus a mean duration of 6.47 Myr (Figure 4). Age model hiatuses do

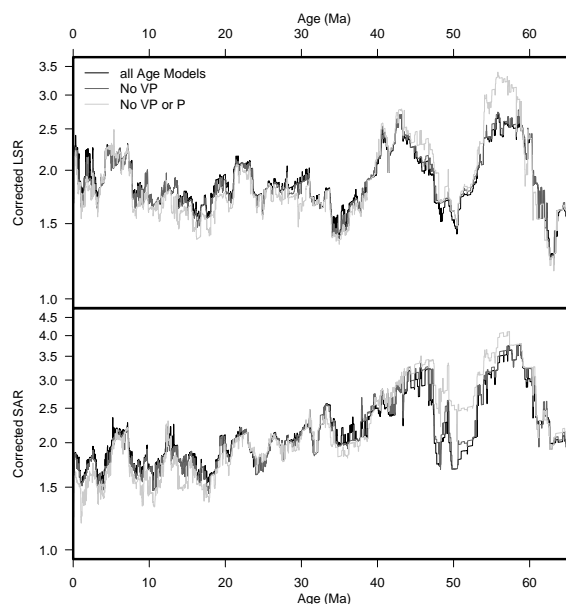


Figure 6. Corrected Linear Sedimentation Rates (top; expressed in $cm.kyr^{-1}$) and Accumulation Rates (bottom panel; expressed in $g.cm^{-2}.kyr^{-1}$). Black: estimates computed using all age model; dark grey: estimates computed after excluding age models of Very Poor (VP) estimated quality; light grey: estimates computed after excluding age models of Very Poor and Poor (P) estimated quality. Rates are on a log-scale.

115 not become more common, or larger, within increasing geologic age, fluctuating $\pm 20\%$ from a mean of ca 22% (Figure 4) (Dutkiewicz and Müller, 2022). Overall, the section age models are on average $> 85\%$ complete (fraction of time represented by sedimentation). Hiatuses thus are insufficient to explain changing apparent SAR. Any change signal therefore must be held in the dominant (sedimenting) part of the sections.

SAR for individual age model segments in the NSB library vary dramatically (< 5 to > 300 m/Myr range; interquartile ratio 120 4.43; Figure 1). By-section normalized rates vary more modestly (interquartile ratio of 2.38); much of the SAR variation thus exists between sections, varying only moderately within a section. Crucially, there is no trend in by-section SAR over geologic time when compiled for the entire dataset (Figure 1): the slope of a linear regression is insignificantly different from zero, and the r^2 is also essentially zero (1.277×10^{-5}). Variations in rate within sections thus are modest, essentially random vs time, and also cannot explain the reported change signal.

125 3.2 Sampling bias by drilling.

In contrast to the above, our model calculating the bias introduced by the drilling process itself shows that, even if sedimentation accumulation rates were perfectly stable through time, we would nonetheless see a major (ca 6X) exponential increase in apparent SAR with decreasing geological age (Figure 2). Further our more comprehensive, NSB-based global compilation of



LSR and SAR (Figure 2) shows that even the apparent (i.e. uncorrected) increase through the Cenozoic is less drastic and more
130 uniform than reported in previous works 4;6. Corrected using our model output for drilling bias, the actual LSR and SAR,
far from increasing throughout the Cenozoic, seem to have decreased slightly (Figure 2), by a factor of 2 (from an estimated
 $4g.cm^{-2}.kyr^{-1}$ in the Paleocene to ca. 2 in the Pleistocene).

This global pattern hides regional disparities. The Pacific Ocean had a relatively stable sedimentation history, with a near
constant early Paleogene SAR that decreased abruptly starting from ca. 41 to 35 Ma, before increasing rapidly shortly before
135 the Eocene-Oligocene boundary to its Cenozoic maxima, followed by a somewhat variable but gradually declining rate to the
Recent. By contrast, the Atlantic Ocean sedimentation history shows a more monotonous decrease throughout the Cenozoic
with two more abrupt decreases: one near the PETM and another one in the Early Miocene. The Indian Ocean shows a decrease
in SAR in the Early Eocene and a short term increase from ca. 40 to 36 Ma. The Southern Ocean is more difficult to interpret
given the very low number of sites, however it seems to show a decrease in SAR at ca. 33 Ma (i. e. near or at the Eocene-
140 Oligocene boundary) and an increase in the earliest Miocene. The latest part of the Antarctic SAR record seems more volatile,
with, in particular, a sharp decrease at ca. 10Ma and another, at ca. 4.8 Ma.

Despite these disparities, the area-corrected global SAR curve (Figure 7) is remarkably close to the global median, and
shares the same characteristics. Apart from its main decreasing trend, it shows a pronounced decrease at ca. 55 Ma, ending at
ca. 49 Ma; and a slower decrease from 42 to 35 Ma, terminating in a fairly sharp increase from 35 to 33 Ma.

145 The global pelagic biogenic sediment flux (Figure 8), correcting for varying area undergoing pelagic biogenic sedimentation
due to changing CCD, shows a near stationary, though slightly decreasing (with a mean around $2.5Pg.yr^{-1}$, ranging from 1.8 to
3.3), Eocene sediment flux, a sharp increase in the latest Eocene from ca. 35.1 Ma to 33.9 Ma, and a net stationary Oligocene
to Recent sediment flux (though marked by wide variations, oscillating from 3.3 to $6.2Pg.yr^{-1}$, around a mean of 4.5).
Although these values are significantly lower than current estimates of Quaternary land-to-sea sediment fluxes (McLennan,
150 1993; Walling and Webb, 1996; Syvitski et al., 2022), our dataset excludes coastal areas, which are dominated by eroded
terrigenous, not chemical weathering produced sediments.

4 Discussion

Uncertainties in our results due to poor age model quality are probably minor given the large number of sites used, and
experience of high stability in biodiversity compilations from the same suite of sections using successive iterations of age
155 model development (Lazarus et al., 2020)(see also Figure 6). Inconsistent coverage by age interval and geographic region may
affect short intervals in our results but are unlikely to significantly affect the basic trends documented. Lastly, CCD trends in
other ocean basins, while not identical (Dutkiewicz and Müller, 2022), largely follow the trend for Pacific CCD, and given the
relative size of basins, differences are not likely to substantially alter the main trend in global flux.

Global mean deep sea pelagic sediment accumulation rates have decreased slightly during the Cenozoic. This contrasts
160 sharply with all previous estimates (Davies et al., 1977; Worsley and Davies, 1979; Hay et al., 1988; Westacott et al., 2021)
which described an increasing trend, in particular in the Neogene. Our result also differs, if less strongly, from the estimate of



constant accumulation between ca 5 and 65 Ma, and higher rates in the last 5 Ma, from seismic data based global sediment thickness maps (Olson et al., 2016). The latter study is not however directly comparable as it includes both terrigenous and biogenic pelagic sediments. Ocean sequestration processes thus have changed over Cenozoic. Despite increasing temperature
165 latitudinal gradients and inferred stronger circulation forcing, both which may have increased ocean turnover, nutrient transfer to surface waters and thus productivity, local sequestration rates have declined. Possible causes are beyond the scope of this paper but could include lower local primary or export productivity, possibly due to lower nutrient concentrations in water, reduced transfer of nutrient waters to surface layers (despite stronger global wind stress) due to increased vertical thermal gradients and stratification, or reduced efficiency of sequestration due to increases in e.g. deep water dissolution. Colder deep
170 oceans since the Oligocene though tend to reduce chemical process rates including dissolution rates – C_{org} (Burdige, 2011); silica (Westacott et al., 2021); carbonates (Morse and Arvidson, 2002) –, thus a reduced efficiency of sequestration seems unlikely.

Adjusting our accumulation rate histories for the changing area of oceans accumulating biogenic sediment however yields a more stationary trend for global biogenic sediment flux to the deep sea, with the difference that the Oligocene to Recent
175 mean is significantly higher than the pre-EOT one. Our results thus largely reconcile the discrepancy that until now has existed between $^{87}Sr/^{86}Sr$ estimates of Cenozoic weathering, and the deep sea pelagic accumulation rate record.

Lastly, although paleoceanographers have long known that older sediments are less commonly recovered than younger ones (Lisitzin, 1996) they have, to our knowledge, largely accepted the recovered record as an unbiased, if ever sparser representation of (older) ocean sediments. Here we show that the Cenozoic deep sea drilling ocean record has a substantial systematic
180 bias. Compilations of paleoceanographic data by time interval need to consider that the older intervals have a substantial over-representation of low sedimentation rate conditions, and an increasingly poor representation of high sedimentation rate environments. This bias may affect a variety of geochemical and micropaleontological synoptic studies that attempt to compare how ocean conditions have changed over the Cenozoic. More broadly, this sampling bias may affect our understanding of any past ocean parameter that varies with either sedimentation rate itself, or with the ocean conditions correlated to sedimentation
185 rate, such as surface water productivity. As these parameters influence a very broad range of ocean processes and chemical cycles (Berger et al., 1989; Morel and Price, 2003; Sarmiento and Gruber, 2006; Hüneke and Henrich, 2011), the discovery of this bias thus will have broad significance, potentially requiring significant reassessment of published literature (Hay et al., 1988; Westacott et al., 2021), as well as affecting the design of many future paleoceanographic and micropaleontologic studies.

5 Conclusions

190 The record of pelagic sedimentation recovered by deep sea drilling is systematically biased. Older time intervals are increasingly represented only by lower accumulation rate sections. This is due to limited total drilling depths and the consequence that reaching older ages happens mostly when drilling in low sedimentation rate sections.



195 The global average accumulation rate in local deep sea pelagic sediment sections has declined slightly over the Cenozoic. As a greater percentage of ocean basins have accumulated sediment over the Cenozoic via deepening of the CCD, the global flux of biogenic sediment has increased, however mostly by a single stepwise increase near the Eocene-Oligocene boundary.

Code and data availability. The code for the model, as well as its output and the data presented here are all available in the Supplementary Materials. Age models are also given in the Supplementary materials while the underlying stratigraphic data are available from the Neptune (NSB) database (Renaudie et al., 2020, 2023).

Author contributions. Both authors conceived the study and wrote the manuscript. DBL wrote the model; JR did the data analysis.

200 *Competing interests.* The authors declare no conflict of interest.

Acknowledgements. This study was funded by the Federal Ministry of Education and Research (BMBF) under the “Make our Planet Great Again – German Research Initiative”, grant number 57429681, implemented by the German Academic Exchange Service (DAAD).



References

- IODP LIMS Reports, <https://web.iodp.tamu.edu/LORE/>, <https://web.iodp.tamu.edu/LORE/>, 2016.
- 205 Berger, W., Smetacek, V., Wefer, G., et al.: Ocean productivity and paleoproductivity—an overview, in: *Productivity of the ocean: present and past*, pp. 1–34, Wiley New York, 1989.
- Burdige, D. J.: Temperature dependence of organic matter remineralization in deeply-buried marine sediments, *Earth and Planetary Science Letters*, 311, 396–410, <https://doi.org/10.1016/j.epsl.2011.09.043>, 2011.
- Coffin, M. F., McKenzie, J., Davis, E., Dickens, G., Ellins, K., Erzinger, J., et al.: Earth, Oceans, and Life. Scientific Investigations of the Earth
210 System using Multiple Drilling Platforms and New Technologies. Integrated Ocean Drilling Program Initial Science Plan, 2003–2013., Integrated Ocean Drilling Program, 2001.
- Cramer, B., Toggweiler, J., Wright, J., Katz, M., and Miller, K.: Ocean overturning since the Late Cretaceous: Inferences from a new benthic foraminiferal isotope compilation, *Paleoceanography*, 24, 2009.
- Dalai, T. K., Ravizza, G. E., and Peucker-Ehrenbrink, B.: The Late Eocene $^{187}\text{Os}/^{188}\text{Os}$ excursion: chemostratigraphy, cosmic dust flux
215 and the early Oligocene glaciation, *Earth and Planetary Science Letters*, 241, 477–492, 2006.
- Davies, T. A., Hay, W. W., Southam, J. R., and Worsley, T. R.: Estimates of Cenozoic oceanic sedimentation rates, *Science*, 197, 53–55, 1977.
- Dutkiewicz, A. and Müller, R. D.: The History of Cenozoic Carbonate Flux in the Atlantic Ocean Constrained by Multiple Regional Carbonate Compensation Depth Reconstructions, *Geochemistry, Geophysics, Geosystems*, 23, e2022GC010667,
220 <https://doi.org/10.1029/2022GC010667>, 2022.
- Glasby, G.: Mineralogy, geochemistry, and origin of Pacific red clays: a review, *New Zealand Journal of Geology and Geophysics*, 34, 167–176, 1991.
- Goddéris, Y. and François, L.: The Cenozoic evolution of the strontium and carbon cycles: relative importance of continental erosion and mantle exchanges, *Chemical Geology*, 126, 169–190, 1995.
- 225 Hay, W. W., Sloan, J. L., and Wold, C. N.: Mass/age distribution and composition of sediments on the ocean floor and the global rate of sediment subduction, *Journal of Geophysical Research: Solid Earth*, 93, 14 933–14 940, 1988.
- Hilgen, F., Lourens, L., Van Dam, J., Beu, A., Boyes, A., Cooper, R., Krijgsman, W., Ogg, J., Piller, W., and Wilson, D.: Chapter 29 - The Neogene Period, in: *The Geologic Time Scale*, edited by Gradstein, F. M., Ogg, J. G., Schmitz, M. D., and Ogg, G. M., pp. 923–978, Elsevier, Boston, ISBN 978-0-444-59425-9, <https://doi.org/https://doi.org/10.1016/B978-0-444-59425-9.00029-9>, 2012.
- 230 Hüneke, H. and Henrich, R.: Pelagic sedimentation in modern and ancient oceans, *Developments in sedimentology*, 63, 215–351, 2011.
- Imbrie, J., Barron, E. J., Berger, W. H., Bornhold, B. D., Sironi, M. B. C., Diester-Haass, L., Elderfield, H., Fischer, A., Lancelot, Y., Prell, W. L., and amd J. Van Hinte, J. R. T.: Scientific goals of an Ocean Drilling Program designed to investigate changes in the global environment., in: *Report of the Second Conference on Scientific Ocean Drilling (COSOD II)*, pp. 15–36, European Science Foundation, 1987.
- 235 Kocsis, Á. T. and Raja, N. B.: chronosphere: Earth system history variables, <http://doi.org/10.5281/zenodo.3530703>, 10.5281/zenodo.3530703, 2020.
- Lazarus, D.: Age depth plot and age maker: Age modelling of stratigraphic sections on the Macintosh series of computers, *Geobyte*, 2, 7–13, 1992.
- Lazarus, D.: Neptune: a marine micropaleontology database, *Mathematical Geology*, 26, 817–832, 1994.



- 240 Lazarus, D., Spencer-Cervato, C., Pika-Biolzi, M., Beckmann, J. P., von Salis, K., Hilbrecht, H., and Thierstein, H.: Revised chronology of Neogene DSDP holes from the world ocean, Ocean Drilling Program Technical Report, 24, 1995.
- Lazarus, D., Suzuki, N., Ishitani, Y., and Takahashi, K.: Paleobiology of the Polycystine Radiolaria, Wiley-Blackwell, 2020.
- Lear, C. H., Elderfield, H., and Wilson, P.: A Cenozoic seawater Sr/Ca record from benthic foraminiferal calcite and its application in determining global weathering fluxes, Earth and Planetary Science Letters, 208, 69–84, 2003.
- 245 Lisiecki, L. E. and Raymo, M. E.: A Pliocene-Pleistocene stack of 57 globally distributed benthic $\delta^{18}O$ records, Paleoceanography, 20, 2005.
- Lisitzin, A. P.: Sedimentation in the World Ocean, vol. 17 of *SEPM Special Publications*, SEPM Society for Sedimentary Geology, 1972.
- Lisitzin, A. P.: Oceanic sedimentation: lithology and geochemistry, American Geophysical Union, 1996.
- McLennan, S. M.: Weathering and global denudation, The Journal of Geology, 101, 295–303, 1993.
- Misra, S. and Froelich, P. N.: Lithium Isotope History of Cenozoic Seawater: Changes in Silicate Weathering and Reverse Weathering, Science, 335, 818–823, <https://doi.org/10.1126/science.1214697>, 2012.
- 250 Mithal, R. and Becker, D. G.: The Janus database: providing worldwide access to ODP and IODP data, Geological Society, London, Special Publications, 267, 253–259, 2006.
- Morel, F. M. and Price, N. M.: The biogeochemical cycles of trace metals in the oceans, Science, 300, 944–947, 2003.
- Morse, J. W. and Arvidson, R. S.: The dissolution kinetics of major sedimentary carbonate minerals, Earth-Science Reviews, 58, 51–84, [https://doi.org/10.1016/S0012-8252\(01\)00083-6](https://doi.org/10.1016/S0012-8252(01)00083-6), 2002.
- 255 National Geophysical Data Center: Core Data from the Deep Sea Drilling Project Legs 1-96. World Data Center for Marine Geology & Geophysics, Seafloor Series, 1, <http://www.ngdc.noaa.gov/mgg/fliers/00mgg03.html>, 2000.
- National Geophysical Data Center: Core Data from the Ocean Drilling Program Legs 101-129. World Data Center for Marine Geology & Geophysics, Seafloor Series, 2, <http://www.ngdc.noaa.gov/mgg/geology/odp/start.htm>, 2001.
- 260 Olson, P., Reynolds, E., Hinnov, L., and Goswami, A.: Variation of ocean sediment thickness with crustal age, Geochemistry, Geophysics, Geosystems, 17, 1349–1369, <https://doi.org/10.1002/2015GC006143>, 2016.
- Pälike, H., Lyle, M. W., Nishi, H., Raffi, I., Ridgwell, A., Gamage, K., Klaus, A., Acton, G., Anderson, L., Backman, J., Baldauf, J., Beltran, C., Bohaty, S. M., Bown, P., Busch, W., Channell, J. E. T., Chun, C. O. J., Delaney, M., Dewangan, P., Dunkley Jones, T., Edgar, K. M., Evans, H., Fitch, P., Foster, G. L., Gussone, N., Hasegawa, H., Hathorne, E. C., Hayashi, H., Herrle, J. O., Holbourn, A., Hovan, S., Hyeong, K., Iijima, K., Ito, T., Kamikuri, S.-i., Kimoto, K., Kuroda, J., Leon-Rodriguez, L., Malinverno, A., Moore Jr, T. C., Murphy, B. H., Murphy, D. P., Nakamura, H., Ogane, K., Ohneiser, C., Richter, C., Robinson, R., Rohling, E. J., Romero, O., Sawada, K., Scher, H., Schneider, L., Sluijs, A., Takata, H., Tian, J., Tsujimoto, A., Wade, B. S., Westerhold, T., Wilkens, R., Williams, T., Wilson, P. A., Yamamoto, Y., Yamamoto, S., Yamazaki, T., and Zeebe, R. E.: A Cenozoic record of the equatorial Pacific carbonate compensation depth, Nature, 488, 609–614, <https://doi.org/10.1038/nature11360>, 2012.
- 265 270 Peucker-Ehrenbrink, B., Ravizza, G., and Hofmann, A.: The marine $^{187}Os/^{188}Os$ record of the past 80 million years, Earth and Planetary Science Letters, 130, 155–167, 1995.
- Raymo, M. E., Ruddiman, W. F., and Froelich, P. N.: Influence of late Cenozoic mountain building on ocean geochemical cycles, Geology, 16, 649–653, 1988.
- Renaudie, J., Lazarus, D. D., and Diver, P.: NSB (Neptune Sandbox Berlin): An expanded and improved database of marine planktonic microfossil data and deep-sea stratigraphy., Palaeontologia Electronica, 23, a11, <https://doi.org/10.26879/1032>, 2020.
- 275 Renaudie, J., Lazarus, D., and Diver, P.: Archive of Neptune (NSB) database backups, <https://doi.org/10.5281/zenodo.10063218>, 2023.



- Ridgwell, A. and Hargreaves, J.: Regulation of atmospheric CO₂ by deep-sea sediments in an Earth system model, *Global Biogeochemical Cycles*, 21, 2007.
- Rothwell, R.: *Sedimentary Rocks: Deep Ocean Pelagic Oozes*, pp. 70–78, Elsevier, ISBN 978-0-12-409548-9, <https://doi.org/10.1016/B978-0-12-409548-9.10493-2>, 2016.
- Sadler, P. M.: Sediment accumulation rates and the completeness of stratigraphic sections, *The Journal of Geology*, 89, 569–584, 1981.
- Sarmiento, J. L. and Gruber, N.: *Ocean Biogeochemical Dynamics*, Princeton University Press, 2006.
- Scotese, C. R. and Wright, N.: PALEOMAP Paleodigital Elevation Models (PaleoDEMS) for the Phanerozoic, <https://www.earthbyte.org/paleodem-resource-scotese-and-wright-2018/>, <https://www.earthbyte.org/paleodem-resource-scotese-and-wright-2018/>, 2018.
- Smith, J., Rillo, M. C., Kocsis, Á. T., Dornelas, M., Fastovich, D., Huang, H.-H. M., Jonkers, L., Kiessling, W., Li, Q., Liow, L. H., Margulis-Ohnuma, M., Meyers, S., Na, L., Penny, A. M., Pippenger, K., Renaudie, J., Saupe, E. E., Steinbauer, M. J., Sugawara, M., Tomašových, A., Williams, J. W., Yasuhara, M., Finnegan, S., and Hull, P. M.: BioDeepTime: A database of biodiversity time series for modern and fossil assemblages, *Global Ecology and Biogeography*, 32, 1680–1689, <https://doi.org/https://doi.org/10.1111/geb.13735>, 2023.
- Syvitski, J., Ángel, J. R., Saito, Y., Overeem, I., Vörösmarty, C. J., Wang, H., and Olago, D.: Earth’s sediment cycle during the Anthropocene, *Nature Reviews Earth & Environment*, 3, 179–196, <https://doi.org/10.1038/s43017-021-00253-w>, 2022.
- Tréguer, P. J. and De La Rocha, C. L.: The world ocean silica cycle, *Annual review of marine science*, 5, 477–501, 2013.
- Tukey, J. W.: *Exploratory data analysis*, Addison-Wesley, Reading, MA, 1977.
- Vandenbergh, N., Hilgen, F., Speijer, R., Ogg, J., Gradstein, F., Hammer, O., Hollis, C., and Hooker, J.: Chapter 28 - The Paleogene Period, in: *The Geologic Time Scale*, edited by Gradstein, F. M., Ogg, J. G., Schmitz, M. D., and Ogg, G. M., pp. 855–921, Elsevier, Boston, ISBN 978-0-444-59425-9, <https://doi.org/https://doi.org/10.1016/B978-0-444-59425-9.00028-7>, 2012.
- Walling, D. and Webb, B.: Erosion and sediment yield: a global overview, in: *Erosion and sediment yield: global and regional perspectives*, edited by Walling, D. and Webb, B., vol. 236, pp. 3–20, IAHS, 1996.
- Westacott, S., Planavsky, N. J., Zhao, M.-Y., and Hull, P. M.: Revisiting the sedimentary record of the rise of diatoms, *Proceedings of the National Academy of Sciences*, 118, e2103517 118, 2021.
- Whitman, J. M. and Davies, T. A.: Cenozoic oceanic sedimentation rates: How good are the data?, *Marine Geology*, 30, 269–284, [https://doi.org/10.1016/0025-3227\(79\)90019-7](https://doi.org/10.1016/0025-3227(79)90019-7), 1979.
- Willenbring, J. K. and Jerolmack, D. J.: The null hypothesis: globally steady rates of erosion, weathering fluxes and shelf sediment accumulation during Late Cenozoic mountain uplift and glaciation, *Terra Nova*, 28, 11–18, <https://doi.org/10.1111/ter.12185>, 2016.
- Worsley, T. R. and Davies, T. A.: Sea-level fluctuations and deep-sea sedimentation rates, *Science*, 203, 455–456, 1979.

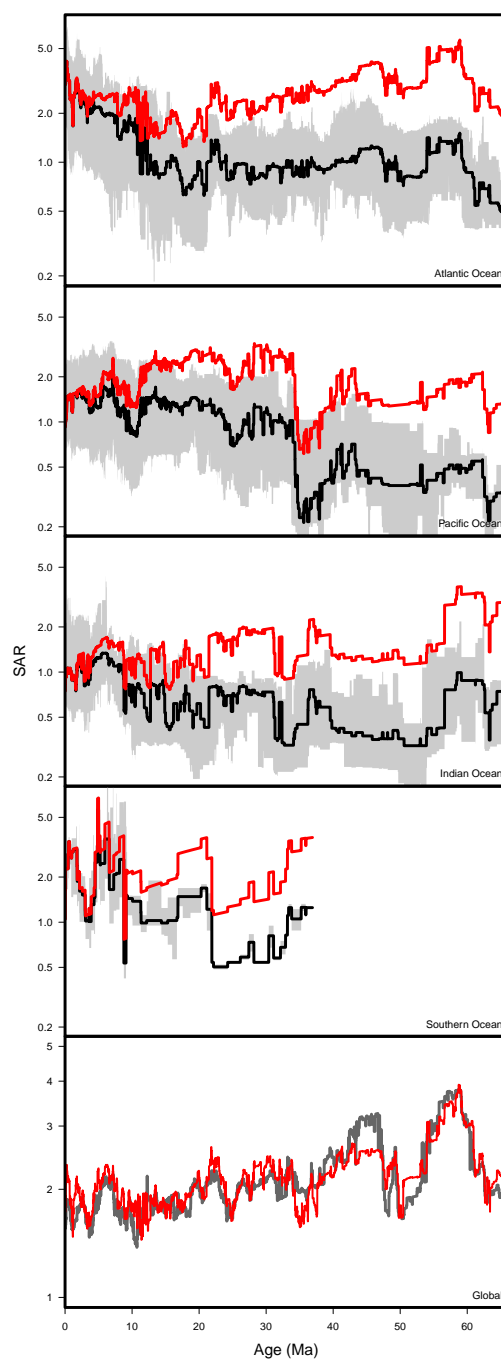


Figure 7. Sediment Accumulation Rates (expressed in $g.cm^{-2}.kyr^{-1}$) distribution observed in each ocean basin (black: median; grey: interquartile range; red: median corrected for drilling bias using the result of the model), shown here on a log-scale. Bottom panel show the weighted global composite based on each basin corrected median value (in red) compared to the corrected but area-unweighted global median SAR shown in Figure 2.

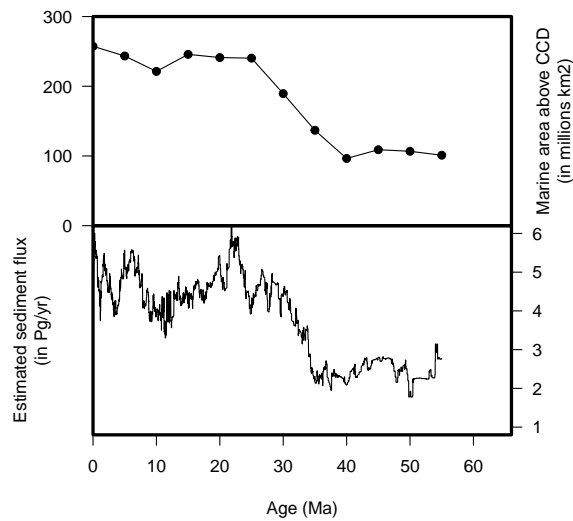


Figure 8. Upper panel: Estimate of changes in the depositional area of pelagic sediments, i. e. area above the Carbonate Compensation Depth (CCD), expressed in millions of km^2 . Calculated from the estimated CCD in the Equatorial Pacific from Pálike et al. (Pálike et al., 2012) and the paleobathymetric maps of Scotese & Wright (Scotese and Wright, 2018; Kocsis and Raja, 2020). Lower panel: Estimated flux of sediments throughout the Cenozoic, expressed in $Pg.yr^{-1}$, based on the composite median SAR of Figure 7 and the changes in depositional area of the panel above.